

Production of charmed baryon $\Lambda_c(2860)$ via low energy antiproton-proton interaction


Qing-Yong Lin^{1,*} and Xiang Liu^{2,3,4,†}

¹*Department of Physics, School of Science, Jimei University, Xiamen 361021, China*

²*School of Physical Science and Technology, Lanzhou University, Lanzhou 730000, China*

³*Lanzhou Center for Theoretical Physics, Key Laboratory of Theoretical Physics of Gansu Province and Frontiers Science Center for Rare Isotopes, Lanzhou University, Lanzhou 730000, China*

⁴*Research Center for Hadron and CSR Physics, Lanzhou University & Institute of Modern Physics of CAS, Lanzhou 730000, China*

 (Received 26 October 2021; revised 30 December 2021; accepted 17 January 2022; published 31 January 2022)

In the present work, we study the production problem of the charmed baryon $\Lambda_c(2860)^+$ at \bar{P} ANDA. With the $J^P = \frac{3}{2}^+$ assignment to $\Lambda_c(2860)^+$, an effective Lagrangian approach is adopted to calculate the cross section of $p\bar{p} \rightarrow \Lambda_c^-\Lambda_c(2860)^+$. The Dalitz plot analysis and the D^0p invariant mass spectrum distribution are also given for the $p\bar{p} \rightarrow \Lambda_c^-\Lambda_c(2860)^+ \rightarrow \Lambda_c^-pD^0$ process. The numerical results show that the total cross section may reach up to about $10 \mu\text{b}$. With the designed luminosity of \bar{P} ANDA ($2 \times 10^{32} \text{ cm}^{-2} \text{ s}^{-1}$), about 10^8 $\Lambda_c(2860)$ events can be expected per day by reconstructing the final pD^0 .

DOI: [10.1103/PhysRevD.105.014035](https://doi.org/10.1103/PhysRevD.105.014035)

I. INTRODUCTION

The charmed baryon family has a special place in whole hadron spectroscopy. Focusing on the charmed baryon, theorists and experimentalists have made a lot of effort to reveal their nature, which has a close relation to constructing the charmed baryon family and finding out the exotic state (see review articles [1–5] for the progress). In the past few years, the charmed baryon family has become more and more abundant with the observation of more excited states of charmed baryon, which can be reflected by the present status of charmed baryons listed in the Particle Data Group (PDG) [6].

Among these observed charmed baryons, $\Lambda_c(2860)^+$ was reported by LHCb in the D^0p channel [7]. The measured mass and width are

$$M = 2856.1_{-1.7}^{+2.0}(\text{stat}) \pm 0.5(\text{syst})_{-5.6}^{+1.1}(\text{model}) \text{ MeV},$$

$$\Gamma = 67.6_{-8.1}^{+10.1}(\text{stat}) \pm 1.4(\text{syst})_{-20.0}^{+5.9}(\text{model}) \text{ MeV},$$

respectively. It should be noted that the uncertainty related to the amplitude model was considered in the analysis

*Corresponding author.
qylin@jmu.edu.cn
†xiangliu@lzu.edu.cn

Published by the American Physical Society under the terms of the [Creative Commons Attribution 4.0 International license](https://creativecommons.org/licenses/by/4.0/). Further distribution of this work must maintain attribution to the author(s) and the published article's title, journal citation, and DOI. Funded by SCOAP³.

presented in the LHCb paper [7]. Thus, when giving the experimental data of mass and width of $\Lambda_c(2860)^+$, this uncertainty was listed. This model uncertainty is marked by (model) in the resonant parameter. Meanwhile, the available experimental analysis indicates that the observed $\Lambda_c(2860)^+$ state has the spin-parity $J^P = \frac{3}{2}^+$. Before the discovery of $\Lambda_c(2860)^+$, many studies were carried out on the mass spectra of charmed baryons with different scenarios and a D -wave charmed baryon with a mass around 2.85 GeV was predicted [8–11], which is consistent with the observation of $\Lambda_c(2860)^+$ from LHCb [7]. Since then, the newly observed $\Lambda_c(2860)^+$ attracted more and more attention from theorists to decode its inner structure and decay property. The Lanzhou group furthermore studied the mass spectrum of the λ -mode excited charmed and charmed-strange baryon states [12]. Their results indicate that $\Lambda_c(2860)^+$ associated with former $\Lambda_c(2880)^+$ can form a D -wave doublet [$3/2^+, 5/2^+$]. More discussions can be found in Refs. [13–17], where different phenomenological methods/models were applied.

Besides the investigation of the mass spectrum, the strong decay properties of the low-lying D -wave charmed baryons were also studied within some methods. The D^0p decay channel is of great importance to provide information on the inner structure of these highly excited Λ_c . The authors carried out the two-body Okubo-Zweig-Iizuka-allowed decays of $\Lambda_c(2860)^+$ within the 3P_0 model and gave the decay widths of different processes [12]. It is obvious that the DN branching fraction reaches up to 95.6%. A smaller value of 75% was obtained with a similar model in Ref. [18]. These results indicate that the DN

channel should be the major decay channel. However, the authors pointed that due to the limited phase space, the partial widths decaying into the DN channel should be small [19].

In addition, the $\Sigma_c\pi$ decay channel should be a channel of concern. However, no signal has been measured for $\Lambda_c(2860)$ experimentally to date. We notice that the partial decay width and the ratio $\mathcal{R} = \frac{\Gamma[\Sigma_c(2520)\pi]}{\Gamma[\Sigma_c(2455)\pi]}$ have been predicted theoretically. The ratio $\mathcal{R} = 0.47$ was predicted in Ref. [12]. Similarly with the 3P_0 model, the authors obtained a value range from 2.8 to 3.0 [20]. By virtue of a constituent quark model, Yao *et al.* got the partial widths to be 4.57 MeV and 0.95 MeV for the decay modes $|{}^2D_{\lambda\lambda}{}^{3+}\rangle \rightarrow \Sigma_c\pi$ and $|{}^2D_{\lambda\lambda}{}^{3+}\rangle \rightarrow \Sigma_c^*\pi$, respectively [21], which leads to a value $\mathcal{R} = 0.21$. Considering the measured width, the relatively large branching fractions indicate that $\Lambda_c(2860)^+$ might be observed in the $\Sigma_c(2455)\pi$ and $\Sigma_c(2520)\pi$ channels as well. In addition, it was pointed out that the ratio \mathcal{R} for the nearby state $\Lambda_c(2880)$ may be strongly affected by $\Lambda_c(2860)$ [21]. Thus, for the purpose of deeply understand $\Lambda_c(2860)$ and other charmed baryons, it is very important to measure the branching ratio. However, the current available information of $\Lambda_c(2860)^+$ is the measured mass and width from the channel decaying to $D^0 p$. Consequently, more experimental information is strongly required to further understand the decay behavior of $\Lambda_c(2860)^+$. The ratio $\mathcal{R} = \frac{\Gamma[\Sigma_c(2520)\pi]}{\Gamma[\Sigma_c(2455)\pi]}$ for the nearby state $\Lambda_c(2880)$ may be strongly affected by $\Lambda_c(2860)$ [21].

Just as reviewed above, the study of $\Lambda_c(2860)^+$ mainly emphasize its mass and decay [8–21]. The discussion of the production of $\Lambda_c(2860)^+$ is still absent. Until now, $\Lambda_c(2860)^+$ was only observed in the Cabibbo-favoured decay $\Lambda_b \rightarrow D^0 p\pi^-$, where another two states $\Lambda_c(2880)^+$ and $\Lambda_c(2940)^+$ previously observed by the *BABAR* experiment [22] were also confirmed [7]. Thus, it is interesting in exploring the $\Lambda_c(2860)^+$ production in other processes. As indicted by the strong decay behavior of $\Lambda_c(2860)^+$ [12,18], the DN decay channel is dominant, which inspires our interesting in exploring the $\Lambda_c(2860)^+$ production via the low energy antiproton-proton interaction. We notice that the future facility \bar{P} ANDA will exploit the annihilation of antiprotons with protons and nuclei to study the fundamental forces in nature [23]. Study of the charmed baryon is one of the main physics goals of \bar{P} ANDA. Some parallel theoretical investigations were previously implemented on the productions of charmed baryons in antiproton-proton collisions [24–27]. The above reason also pushes us to study the discovery potential of $\Lambda_c(2860)^+$ at \bar{P} ANDA, which can provide valuable information to future experimental exploration of $\Lambda_c(2860)^+$ at \bar{P} ANDA.

This work is organized as follows. After the Introduction, we present the theoretical model and the corresponding calculation details in Sec. II. The numerical results of the $\Lambda_c(2860)^+$ production at \bar{P} ANDA will be

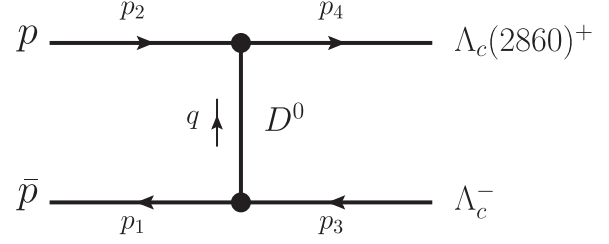


FIG. 1. The diagram describing the $\bar{p}p \rightarrow \Lambda_c^-\Lambda_c(2860)^+$ process.

given in Sec. III, including the cross sections, the Dalitz plot, and the pD^0 invariant mass spectrum. Finally, this paper ends with a discussion and conclusion (see Sec. IV).

II. $\Lambda_c(2860)$ PRODUCTION IN $\bar{p}p$ ANNIHILATION

As discussed above, $\Lambda_c(2860)^+$ could be produced in the antiproton and proton collision by exchanging a D^0 meson, as shown in Fig. 1. It should be noted that the $p\bar{p}$ annihilation (s channel) is an Okubo-Zweig-Iizuka (OZI) suppressed process. Thus, the contribution from the annihilation channel can be negligible compared with the contribution from the t channel shown in Fig. 1. In our calculation, only the t channel is considered.

Before evaluating the cross section of $\bar{p}p \rightarrow \Lambda_c^-\Lambda_c(2860)^+$, we display the kinematically allowed region of the square of the transfer momentum q^2 in Fig. 2, which is the function of the center-of-mass (c.m.) energy \sqrt{s} . As shown in Fig. 2, the maximum of q^2 is negative and less than the mass square of the exchanged D^0 meson in the energy range of our interest.

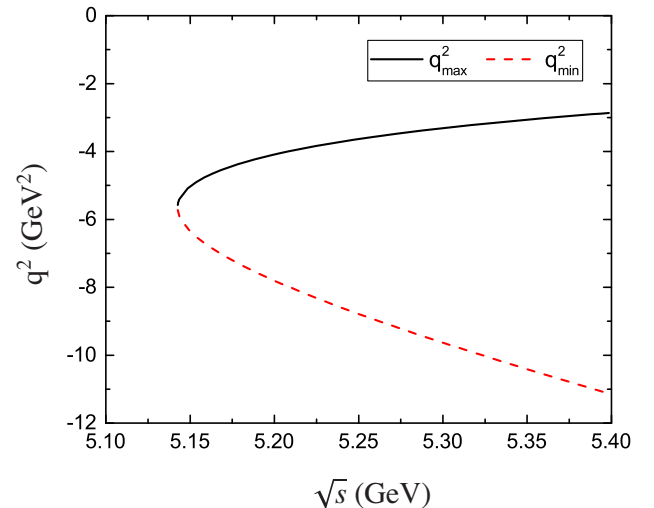


FIG. 2. The kinematically allowed region for the momentum of the transfer momentum in the processes $p\bar{p} \rightarrow \Lambda_c(2860)^+\Lambda_c^-$.

A. The formalism

The effective Lagrangian approach is utilized to study the $\bar{p}p \rightarrow \bar{\Lambda}_c \Lambda_c(2860)^+$ process. As measured by LHCb [7], we take the quantum number of $\Lambda_c(2860)^+$ to be $J^P = 3/2^+$. To describe the interaction of the nucleon with the charmed meson and the charmed baryon, we adopt the following effective Lagrangians [24,28–32]

$$\mathcal{L}_{Dp\Lambda_c} = g_{Dp\Lambda_c} \bar{\Lambda}_c i\gamma_5 D^0 p + \text{H.c.}, \quad (1)$$

$$\mathcal{L}_{D^*p\Lambda_c} = g_{D^*p\Lambda_c} \bar{\Lambda}_c \gamma^\mu D_\mu^* p + \text{H.c.}, \quad (2)$$

$$\mathcal{L}_{DN\Sigma_c} = -g_{DN\Sigma_c} \bar{N} i\gamma_5 \boldsymbol{\tau} \cdot \boldsymbol{\Sigma}_c \bar{D} + \text{H.c.}, \quad (3)$$

$$\mathcal{L}_{D^*N\Sigma_c} = g_{D^*N\Sigma_c} \bar{N} \gamma^\mu \boldsymbol{\tau} \cdot \boldsymbol{\Sigma}_c \bar{D}_\mu^* + \text{H.c.}, \quad (4)$$

$$\mathcal{L}_{DpR} = g_{DpR} \bar{R} \partial_\mu D^0 p + \text{H.c.}, \quad (5)$$

where p/N , Λ_c , Σ_c , R , D^0 , and D^{*0} denote the proton/nucleon, $\Lambda_c(2286)^+$, $\Sigma_c(2455)^+$, $\Lambda_c(2860)^+$, D^0 , and D^{*0} fields, respectively. In the following formulas, the abbreviations $g_{\Lambda_c} \equiv g_{Dp\Lambda_c}$, $g'_{\Lambda_c} \equiv g_{D^*p\Lambda_c}$, $g_{\Sigma_c} \equiv g_{DN\Sigma_c}$, $g'_{\Sigma_c} \equiv g_{D^*N\Sigma_c}$, and $g_R \equiv g_{DpR}$ are implemented. The coupling constants $g_{\Lambda_c} = -13.98$, $g'_{\Lambda_c} = -5.20$, $g_{\Sigma_c} = -2.69$, $g'_{\Sigma_c} = 3.0$ are determined from the SU(4) invariant Lagrangians in terms of $g\pi NN = 13.45$ and $g_{\rho NN} = 6.0$ [28–30]. The coupling constant g_R will be discussed later.

The propagators for the fermion with $J = 1/2$, and $3/2$ are expressed as [32–35]

$$G_{\mathcal{F}}^{n+(1/2)}(p) = P^{(n+(1/2))}(p) \frac{i2m_{\mathcal{F}}}{p^2 - m_{\mathcal{F}}^2 + im_{\mathcal{F}}\Gamma_{\mathcal{F}}} \quad (6)$$

with

$$P^{1/2}(p) = \frac{\not{p} + m_{\mathcal{F}}}{2m_{\mathcal{F}}}, \quad (7)$$

$$P^{3/2}(p) = \frac{\not{p} + m_{\mathcal{F}}}{2m_{\mathcal{F}}} Q_{\mu\nu}(p), \quad (8)$$

$$Q_{\mu\nu}(p) = -g_{\mu\nu} + \frac{1}{3}\gamma_\mu \gamma_\nu + \frac{1}{3m_{\mathcal{F}}}(\gamma_\mu p_\nu - \gamma_\nu p_\mu) + \frac{2}{3m_{\mathcal{F}}^2} p_\mu p_\nu, \quad (9)$$

where p and $m_{\mathcal{F}}$ are momentum and mass of the fermion, respectively. The propagators for the exchanged D^0 and D^{*0} are written as

$$G_D(q^2) = \frac{i}{q^2 - m_D^2} \quad (10)$$

$$G_{D^{*0}}(q^2) = \frac{i(-g^{\mu\nu} + \frac{q^\mu q^\nu}{q^2})}{q^2 - m_{D^{*0}}^2}. \quad (11)$$

In the effective Lagrangian approach, the cross section of $p\bar{p} \rightarrow \bar{\Lambda}_c \Lambda_c(2860)^+$ is proportional to g_R^2 and the line shape depends on the c.m. energy. Here, a concrete g_R value is adopted to execute the calculations. Generally, the coupling constant g_R can be obtained by fitting the measured partial width of the $\Lambda_c(2860)^+(k) \rightarrow D^0(q)p(p)$ decay, where the partial decay width is

$$d\Gamma_i = \frac{m_R m_N}{8\pi^2} |\mathcal{M}|^2 \frac{|\vec{q}|}{m_R^2} d\Omega \quad (12)$$

with

$$E_q = \frac{m_R^2 - m_N^2 + m_D^2}{2m_R}, \quad (13)$$

$$|\vec{q}| = \frac{\sqrt{[m_R^2 - (m_D + m_N)^2][m_R^2 - (m_D - m_N)^2]}}{2m_R}. \quad (14)$$

Here, E_q and \vec{q} denote the energy and the three-momentum of the daughter D^0 meson, respectively. m_N and m_D are the masses of proton and D^0 meson, respectively. Furthermore, the concrete expression of the corresponding decay width is

$$\begin{aligned} \Gamma_i &= \frac{g_R^2 m_N |\vec{q}|}{8\pi} \sum \text{Tr}[u(p)\bar{u}(p)q_\mu u_R^\mu(k)\bar{u}_R^\nu(k)q_\nu] \\ &= \frac{g_R^2 |\vec{q}|}{16\pi m_R} \text{Tr}[(\not{p} + m_N)\tilde{P}^{3/2}(k)q_\mu q_\nu], \end{aligned} \quad (15)$$

where $P^{3/2}(k)$ is the projection operator for a fermion with $J = 3/2$ as defined in Eq. (8). Until now, the branching ratio of $\Lambda_c(2880)^+ \rightarrow D^0 p$ is still not measured experimentally. We notice that the branching ratio of $\Lambda_c(2860)^+ \rightarrow D^0 p$ has been theoretically predicted in several previous work. Thus it is feasible to determine the coupling constant g_R by the theoretical result, where the branching fraction $\text{BR}(\Lambda_c(2860)^+ \rightarrow D^0 p) = 48\%$ estimated in Ref. [12] is adopted. Considering the above situation, in this work we extract $g_R = 10.25 \text{ GeV}^{-1}$ by taking a typical value $\Gamma(\Lambda_c(2860)^+ \rightarrow D^0 p) = 32.4 \text{ MeV}$. In addition, the discussion for the contribution of the width uncertainty is necessary. By considering the experimental systematic and model uncertainties, one may obtain the uncertainty to be $^{+7.3}_{-18.6} \text{ MeV}$ on the total width. Here, we find that the positive one $+7.3 \text{ MeV}$ is about ten percent of the total width 67.6 MeV . To estimate the effect of the uncertainties of the coupling constant on the cross section, we suppose the total width has a margin of error of plus or minus 10 percentage points. The value of g_R is in the range of

9.73–10.76 GeV⁻¹. These results are applied to the following calculations.

Additionally, since the hadrons are not pointlike particles, the monopole form factor [24,30]

$$\mathcal{F}_M(q^2, m^2) = \frac{\Lambda^2 - m^2}{\Lambda^2 - q^2} \quad (16)$$

is introduced to phenomenologically describe the inner structure effect of the interaction vertices and compensates the off-shell effect for the t channel with the D^0 or D^{*0} meson exchange. Meanwhile, a form factor [36]

$$\mathcal{F}_B(q^2, m^2) = \frac{\Lambda^4}{\Lambda^4 + (q^2 - m^2)^2} \quad (17)$$

is also employed for the intermediate baryons. Here, the q and m denote the four-momentum and mass of the exchanged hadron, respectively. The cutoff Λ will be discussed below.

B. The cross section of $p\bar{p} \rightarrow \Lambda_c^- \Lambda_c^+(2860)^+$

The transition amplitude for the process $p\bar{p} \rightarrow \Lambda_c^- \Lambda_c^+(2860)^+$ as shown in Fig. 1 can be expressed as

$$\begin{aligned} \mathcal{M} = & \bar{u}_R(p_4) \mathcal{V}_R(q) u_p(p_2) \bar{v}_{\bar{p}}(p_1) \mathcal{V}(q) v_{\Lambda_c}(p_3) \\ & \times G_D(q^2) \mathcal{F}_M^2(q^2, m_D^2), \end{aligned} \quad (18)$$

where p_1, p_2, p_3, p_4 , and q are the momenta of $\bar{p}, p, \Lambda_c, \Lambda_c(2860)^+$, and the exchanged D^0 meson, respectively. \mathcal{V}_R or \mathcal{V} describes the Lorentz structure of the $\Lambda_c(2860)^+ p D^0$ or $\bar{\Lambda}_c \bar{p} D^0$ interaction vertex including coupling constant. They can be derived by virtue of the Lagrangians in Eqs. (1) and (5).

The unpolarized cross section is [6]

$$\frac{d\sigma}{dt} = \frac{m_N m_N m_{\Lambda_c} m_R}{16\pi s} \frac{1}{|\vec{p}_1|^2} \sum |\mathcal{M}|^2, \quad (19)$$

where

$$\begin{aligned} \sum |\mathcal{M}|^2 = & |G_D(q^2)|^2 \mathcal{F}_M^4(q^2, m_D^2) \\ & \times \text{Tr} \left[P^{3/2}(p_4) \mathcal{V}_R(q) \frac{\not{p}_2 + m_N}{2m_N} \gamma^0 \mathcal{V}_R(q)^\dagger \gamma^0 \right] \\ & \times \text{Tr} \left[\frac{\not{p}_1 - m_N}{2m_N} \mathcal{V} \frac{\not{p}_3 - m_{\Lambda_c}}{2m_{\Lambda_c}} \gamma^0 \mathcal{V}^\dagger \gamma^0 \right]. \end{aligned} \quad (20)$$

Before studying the cross section for the $\Lambda_c(2860)^+$, it is necessary to calculate the total cross section for the reaction $p\bar{p} \rightarrow \Lambda_c^- \Lambda_c^+$. It is of great importance for the background analyses. The transition amplitude of $p\bar{p} \rightarrow \Lambda_c^- \Lambda_c^+$ can be obtained by replacing $\mathcal{V}_R(q)$ with $\mathcal{V}(q)$ in Eq. (18). In Fig. 3, the total cross section of $p\bar{p} \rightarrow \Lambda_c^- \Lambda_c^+$ with different

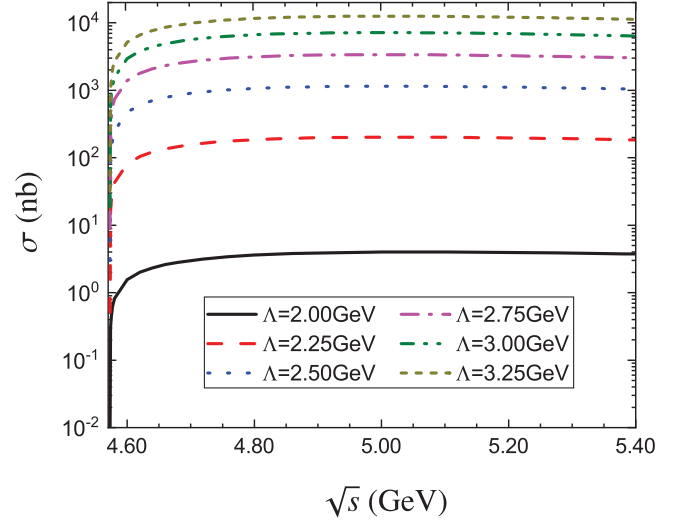


FIG. 3. The obtained total cross section for $p\bar{p} \rightarrow \Lambda_c^- \Lambda_c^+$ with different cutoff values.

cutoff values is presented. The cutoff Λ in the form factor is a phenomenological parameter and we restrict the Λ value within a reasonable range from 2.00 GeV to 3.25 GeV.

With the similar consideration, the cross sections for the production of $\Lambda_c(2860)^+$ with different cutoffs are presented in Fig. 4. Our results indicate that the cross section strongly depends on the values of Λ . The cross section with $\Lambda = 2.00$ is much smaller than that with $\Lambda = 3.25$ by a fraction of $\sim 10^4$. In addition, the cross section of $p\bar{p} \rightarrow \Lambda_c^- \Lambda_c^+$ is smaller than that of $p\bar{p} \rightarrow \Lambda_c^- \Lambda_c^+(2860)^+$ if taking a same cutoff. This is mainly due to the reason that the exchanged Λ_c^+ is off-shell while the $\Lambda_c^+(2860)$ can be on-shell.

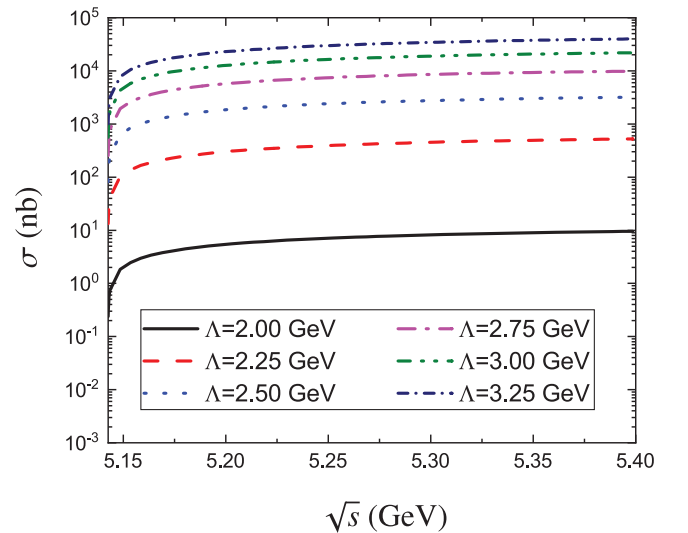


FIG. 4. The obtained total cross section for $p\bar{p} \rightarrow \Lambda_c^- \Lambda_c^+(2860)^+$ with different cutoffs.

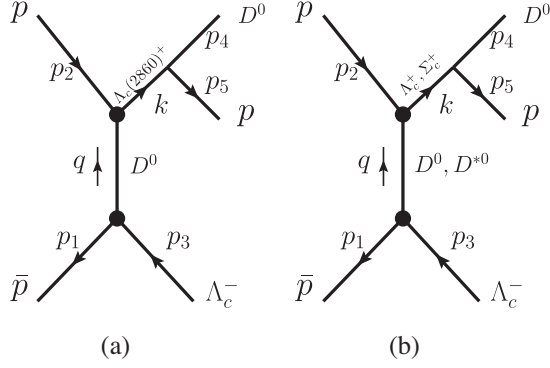


FIG. 5. The diagrams for $p\bar{p} \rightarrow D^0 p \bar{\Lambda}_c$ with different intermediate particles. (a) The signal channel with exchanged D^0 meson and intermediate $\Lambda_c(2860)^+$ contributions. (b) The background with exchanged D^0/D^{*0} mesons and intermediate Λ_c/Σ_c contributions.

In Ref. [24], the production of $\Lambda_c(2940)^+$ via the $\bar{p}p$ collision was studied, where the cutoff was set to be 3 GeV. Considering the obvious similarity between these reactions, we adopt the same value to estimate the production rate of $\Lambda_c(2860)^+$ in the $\bar{p}p$ reaction. In addition, we use other cutoff parameters $\Lambda_{D^*} = \Lambda_{\Lambda_c} = \Lambda_{\Lambda_c^*} = \Lambda_{\Sigma_c} = \Lambda = 3.0$ GeV for minimizing the free parameters.

III. THE BACKGROUND ANALYSIS

The background analysis and invariant mass spectrum are also important for the study of $\Lambda_c(2860)^+$ production in $\bar{p}p$ reaction. They may give more information for the corresponding reaction. In this section, we present Dalitz plot and pD^0 invariant mass spectrum for the reaction $p\bar{p} \rightarrow \Lambda_c^- \Lambda_c(2860)^+$ as shown in Fig. 5, where the intermediate states $\Lambda_c(2860)^+$, $\Lambda_c(2286)^+$, and $\Sigma_c(2455)^+$ are involved. The processes $p\bar{p} \rightarrow \Lambda_c^- \Lambda_c^+ \rightarrow \Lambda_c^- p D^0$ and $p\bar{p} \rightarrow \Lambda_c^- \Sigma_c^+ \rightarrow \Lambda_c^- p D^0$ with both D^0 and D^{*0} exchanges are as the main background contributions.

The transition amplitude of $p\bar{p} \rightarrow \Lambda_c^- \Lambda_c(2860)^+ \rightarrow \Lambda_c^- p D^0$ is written as

$$\begin{aligned} \mathcal{M}_a = & \bar{u}_p(p_4) \mathcal{V}_R(p_5) G_R^{3/2}(k) \mathcal{V}_R(q) u_p(p_2) G_D(q^2) \\ & \times \bar{v}_{\Lambda_c^-}(p_3) \mathcal{V}_{\Lambda_c}(q) v_{\bar{p}}(p_1) \mathcal{F}_M^2(q^2, M_D^2) \\ & \times \mathcal{F}_B(k^2, M_R^2), \end{aligned} \quad (21)$$

The involved momenta are defined in Fig. 5. One can easily obtain the amplitudes of the other four processes, as shown in Fig. 5(b), by replacing the relevant masses, form factors, propagators, and vertices which can be derived from Eqs. (1)–(5). Here, the sum of the four amplitudes is expressed as \mathcal{M}_b .

With the above amplitudes, the square of the total invariant transition amplitude reads as

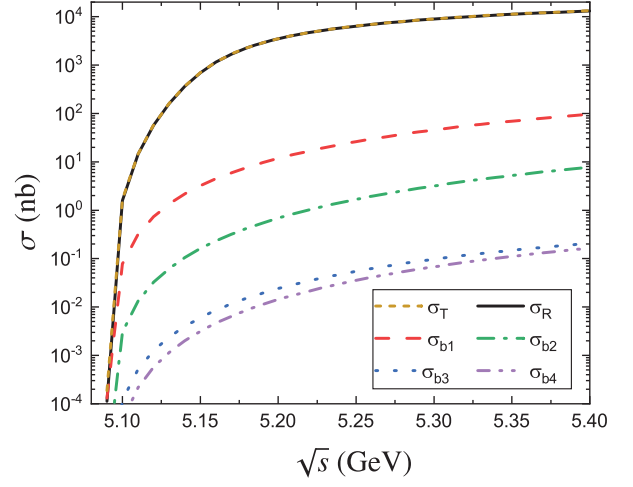


FIG. 6. The obtained total cross section for $p\bar{p} \rightarrow \Lambda_c^- p D^0$ with $g_R = 10.25$ GeV $^{-1}$.

$$|\mathcal{M}|^2 = \sum |\mathcal{M}_a + \mathcal{M}_b|^2. \quad (22)$$

The corresponding total cross section of the process $p\bar{p} \rightarrow \Lambda_c^- p D^0$ is

$$d\sigma = \frac{m_N^2}{|p_1 \cdot p_2|} \frac{|\mathcal{M}|^2}{4} (2\pi)^4 d\Phi_3(p_1 + p_2; p_3, p_4, p_5) \quad (23)$$

with the definition of n -body phase space [6]

$$d\Phi_n(P; k_1, \dots, k_n) = \delta^4\left(P - \sum_{i=1}^n k_i\right) \prod_{i=1}^n \frac{d^3 k_i}{(2\pi)^3 2E_i}. \quad (24)$$

In Fig. 6, the total cross section is given, which is dependent on \sqrt{s} . Here, σ_R and σ_T correspond to the signal and total cross section, respectively. σ_{b1} and σ_{b2} correspond to that of $p\bar{p} \rightarrow \Lambda_c^- \Lambda_c^+ \rightarrow \Lambda_c^- p D^0$ with D^0 and D^{*0} exchanges, respectively. σ_{b3} and σ_{b4} correspond to that of $p\bar{p} \rightarrow \Lambda_c^- \Sigma_c^+ \rightarrow \Lambda_c^- p D^0$ with D^0 and D^{*0} exchanges, respectively. As shown in Fig. 6, $\sigma_{b1} + \sigma_{b2}$ is much larger than $\sigma_{b3} + \sigma_{b4}$, which indicates that the reaction $p\bar{p} \rightarrow \Lambda_c^- p D^0$ via the intermediate Λ_c^+ should be the main

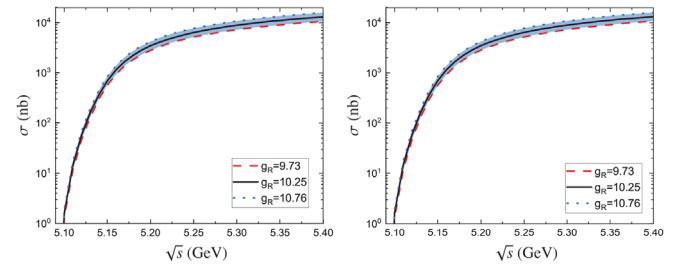


FIG. 7. The obtained total cross section for $p\bar{p} \rightarrow \Lambda_c^- p D^0$ with different g_R . The left and right figures correspond to σ_R and σ_T , respectively.

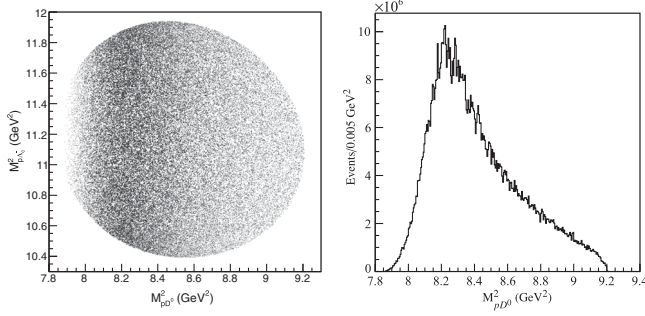


FIG. 8. The Dalitz plot (left) and pD^0 invariant mass spectrum distribution (right) for $p\bar{p} \rightarrow \Lambda_c^- pD^0$ at $\sqrt{s} = 5.32$ GeV.

background. One can also find that σ_{b1} reaches up to about 100 nb at $\sqrt{s} = 5.4$ GeV, which is about one order of magnitude larger than σ_{b2} . Thus the main contribution to the background comes from the reaction $p\bar{p} \rightarrow \Lambda_c^- \Lambda_c^+ \rightarrow \Lambda_c^- pD^0$ with the D^0 exchange. The cross section for the production of $\Lambda_c(2860)^+$ increases rapidly near the threshold and then reaches up to about $13 \mu\text{b}$ at $\sqrt{s} = 5.4$ GeV. The results indicate that the signal can be easily distinguished from the background. In addition, if the total width of $\Lambda_c(2860)$ has an uncertainty of 10%, the coupling constant g_R is the range of $9.73\text{--}10.76 \text{ GeV}^{-1}$. The corresponding cross sections with these different g_R values are shown in Fig. 7.

With the help of *Mathematica* and FOWL codes, we present the Dalitz plot for the $p\bar{p} \rightarrow \Lambda_c^- pD^0$ process and the pD^0 invariant mass spectrum at $\sqrt{s} = 5.32$ GeV in Fig. 8.

IV. SUMMARY

In this work, we investigate the production of the charmed baryon $\Lambda_c(2860)$ via antiproton-proton reaction, which is different from the $\Lambda_c(2860)$ production observed in the Λ_b^0 decay [7]. The present study can supply valuable information for the experimental search for $\Lambda_c(2860)$ in the future experiments at PANDA [23].

It should be noted that the initial state interaction (ISI) and final state interaction (FSI) may play an important role on the nucleon-nucleon entrance channel [37–40]. However, the ISI and FSI effects are thought to be described by the nonperturbative QCD and should be rather complicated. We notice that the authors in Refs. [37,39] studied the ISI effects on nucleon collisions. Their results indicate that the ISI leads to a suppression on the cross section, which may change the cross section by a factor no more than 10%–15%. Furthermore, with the frame of the Jülich meson-baryon model [40], the FSI effect on the cross section was implemented. However, the aim of the present work is to carry out the discovery potential of $\Lambda_c(2860)$ produced at PANDA. The ISI and FSI effects are rather complicated and go beyond the scope

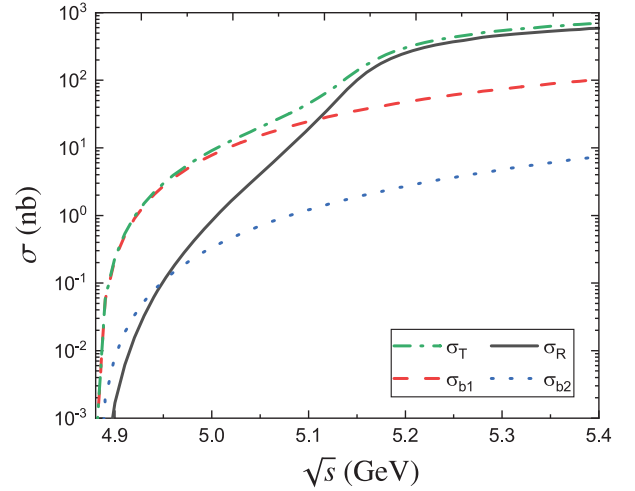


FIG. 9. The obtained total cross section for $p\bar{p} \rightarrow \Lambda_c^- \Sigma_c^{++} \pi^-$ with $(g_R, g_R') = (10.25, 1.01)$.

of this work. Therefore, as suggested by previous research [24,38], a reasonable factor is introduced to reflect the ISI effect, which makes the cross section of $p\bar{p} \rightarrow \Lambda_c^- \Lambda_c(2860)^+$ suppressed by 1 order of magnitude (this factor is considered for the above calculations). With the above consideration, one can roughly estimate the events of $\Lambda_c(2860)$ produced at PANDA. Considering the designed luminosity of PANDA ($2 \times 10^{32} \text{ cm}^{-2} \text{ s}^{-1}$), one may expect that there are about 10^8 $\Lambda_c(2860)$ events accumulated per day by reconstructing the final pD^0 . The Dalitz plot and pD^0 invariant mass spectrum analyses are also performed. We find that the signal can be easily distinguished from the background.

Inspired by the theoretical predictions [12,20,21], we also study the $\Lambda_c(2860)$ production in $p\bar{p} \rightarrow \Lambda_c^- \Sigma_c^{++} \pi^-$. Here, $p\bar{p} \rightarrow \Lambda_c^- \Lambda_c(2860)^+ \rightarrow \Lambda_c^- \Sigma_c^{++} \pi^-$ and $p\bar{p} \rightarrow \Lambda_c^- \Lambda_c^+ \rightarrow \Lambda_c^- \Sigma_c^{++} \pi^-$ correspond to the signal and background channel, respectively. For the background channel, the contributions are both from D^0 and D^{*0} exchanges, which are labeled as σ_{b1} and σ_{b2} in Fig. 9. The cross section with $\text{BR}(\Lambda_c(2860)^+ \rightarrow \Sigma_c^{++} \pi^-) \sim 3.0\%$ is presented in Fig. 9, where the coupling constant $g_{\Lambda_c \Sigma_c \pi} = 9.32$ is

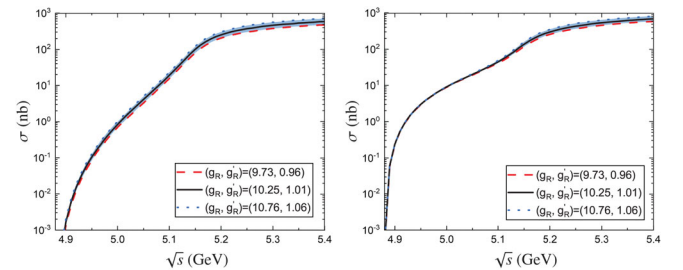


FIG. 10. The obtained total cross section for $p\bar{p} \rightarrow \Lambda_c^- \Sigma_c^{++} \pi^-$ with different g_R and g_R' . The left and right figures correspond to σ_R and σ_T , respectively.

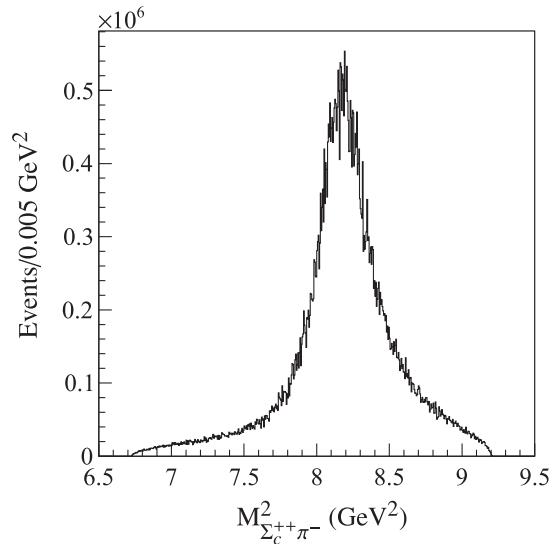


FIG. 11. The $\Sigma_c^{++}\pi^-$ invariant mass spectrum distribution for $p\bar{p} \rightarrow \Lambda_c^-\Sigma_c^{++}\pi^-$ at $\sqrt{s} = 5.32$ GeV.

adopted [30]. As discussed above, the uncertainties of the coupling constants g_R and $g'_R \equiv g_{R\Sigma_c\pi}$ are also considered, with g'_R varying from 0.96 to 1.06 GeV $^{-1}$. The corresponding results are shown in Fig. 10. The invariant mass spectrum of $\Sigma_c^{++}\pi^-$ is also simulated and presented in Fig. 11. As shown in Figs. 9 and Fig. 11, the signal is

several times larger than the background and can be distinguished clearly. Thus, the channel $p\bar{p} \rightarrow \Lambda_c^-\Sigma_c^{++}\pi^-$ is also a suitable channel to study $\Lambda_c(2860)$. Due to the small branching fraction, we do not consider the contribution from $\Sigma_c(2520)\pi$ channel.

In addition, as discussed in Ref. [21], the ratio $\mathcal{R} = \frac{\Gamma[\Sigma_c(2520)\pi]}{\Gamma[\Sigma_c(2455)\pi]}$ for the nearby state $\Lambda_c(2880)$ may be strongly affected by $\Lambda_c(2860)$. Thus, it is an interesting topic to study the $p\bar{p} \rightarrow \Lambda_c^-\Sigma_c(2455)^{++}\pi^-$ and $p\bar{p} \rightarrow \Lambda_c^-\Sigma_c(2520)^{++}\pi^-$ reactions within the contributions from both $\Lambda_c(2860)$ and $\Lambda_c(2880)$, which can be accessible at future experiment like PANDA.

ACKNOWLEDGMENTS

This project is supported by the National Natural Science Foundation of China (Grant No. 11747160), the Natural Science Foundation of Fujian Province (Grant No. 2018J05007) and the Scientific Research Foundation of Jimei University (Grant No. ZQ2017007). X.L. is supported by the China National Funds for Distinguished Young Scientists under Grant No. 11825503, National Key Research and Development Program of China under Contract No. 2020YFA0406400, the 111 Project under Grant No. B20063, and the National Natural Science Foundation of China under Grant No. 12047501.

-
- [1] E. Klempt and J. M. Richard, *Rev. Mod. Phys.* **82**, 1095 (2010).
- [2] H. X. Chen, W. Chen, X. Liu, Y. R. Liu, and S. L. Zhu, *Rep. Prog. Phys.* **80**, 076201 (2017).
- [3] F. K. Guo, C. Hanhart, U. G. Meißner, Q. Wang, Q. Zhao, and B. S. Zou, *Rev. Mod. Phys.* **90**, 015004 (2018).
- [4] Y. Kato and T. Iijima, *Prog. Part. Nucl. Phys.* **105**, 61 (2019).
- [5] V. O. Galkin and R. N. Faustov, *Phys. Part. Nucl.* **51**, 661 (2020).
- [6] P. A. Zyla *et al.* (Particle Data Group), *Prog. Theor. Exp. Phys.* (2020), 083C01.
- [7] R. Aaij *et al.* (LHCb Collaboration), *J. High Energy Phys.* **05** (2017) 030.
- [8] B. Chen, K. W. Wei, and A. Zhang, *Eur. Phys. J. A* **51**, 82 (2015).
- [9] B. Chen, K. W. Wei, X. Liu, and T. Matsuki, *Eur. Phys. J. C* **77**, 154 (2017).
- [10] Q. F. Lü, Y. Dong, X. Liu, and T. Matsuki, *Nucl. Phys. Rev.* **35**, 1 (2018).
- [11] H. X. Chen, Q. Mao, A. Hosaka, X. Liu, and S. L. Zhu, *Phys. Rev. D* **94**, 114016 (2016).
- [12] B. Chen, X. Liu, and A. Zhang, *Phys. Rev. D* **95**, 074022 (2017).
- [13] Z. G. Wang, *Nucl. Phys.* **B926**, 467 (2018).
- [14] Q. Mao, H. X. Chen, A. Hosaka, X. Liu, and S. L. Zhu, *Int. J. Mod. Phys. Conf. Ser.* **46**, 1860083 (2018).
- [15] R. N. Faustov and V. O. Galkin, *EPJ Web Conf.* **204**, 08001 (2019).
- [16] K. Gandhi, Z. Shah, and A. K. Rai, *Int. J. Theor. Phys.* **59**, 1129 (2020).
- [17] B. Chen, S. Q. Luo, and X. Liu, *Eur. Phys. J. C* **81**, 474 (2021).
- [18] K. Gong, H. Y. Jing, and A. Zhang, *Eur. Phys. J. C* **81**, 467 (2021).
- [19] Q. F. Lü and X. H. Zhong, *Phys. Rev. D* **101**, 014017 (2020).
- [20] J. J. Guo, P. Yang, and A. Zhang, *Phys. Rev. D* **100**, 014001 (2019).
- [21] Y. X. Yao, K. L. Wang, and X. H. Zhong, *Phys. Rev. D* **98**, 076015 (2018).
- [22] B. Aubert *et al.* (BABAR Collaboration), *Phys. Rev. Lett.* **98**, 012001 (2007).
- [23] M. F. M. Lutz *et al.* (PANDA Collaboration), arXiv:0903.3905.
- [24] J. He, Z. Ouyang, X. Liu, and X. Q. Li, *Phys. Rev. D* **84**, 114010 (2011).

- [25] Q. Y. Lin, X. Liu, and H. S. Xu, *Phys. Rev. D* **90**, 014014 (2014).
- [26] R. Shyam, *Phys. Rev. D* **96**, 116019 (2017).
- [27] J. Haidenbauer and G. Krein, *Phys. Rev. D* **95**, 014017 (2017).
- [28] Y. Dong, A. Faessler, T. Gutsche, and V. E. Lyubovitskij, *Phys. Rev. D* **81**, 014006 (2010).
- [29] Y. Dong, A. Faessler, T. Gutsche, S. Kumano, and V. E. Lyubovitskij, *Phys. Rev. D* **82**, 034035 (2010).
- [30] J. J. Xie, Y. B. Dong, and X. Cao, *Phys. Rev. D* **92**, 034029 (2015).
- [31] Y. Huang, J. He, J. J. Xie, and L. S. Geng, *Phys. Rev. D* **99**, 014045 (2019).
- [32] J.-J. Wu, Z. Ouyang, and B. S. Zou, *Phys. Rev. C* **80**, 045211 (2009).
- [33] R. Machleidt, K. Holinde, and C. Elster, *Phys. Rep.* **149**, 1 (1987).
- [34] K. Tsushima, A. Sibirtsev, A. W. Thomas, and G. Q. Li, *Phys. Rev. C* **59**, 369 (1999); **61**, 029903(E) (2000).
- [35] S.-Z. Huang, P.-F. Zhang, T.-N. Ruan, Y.-C. Zhu, and Z.-P. Zheng, *Eur. Phys. J. C* **42**, 375 (2005).
- [36] V. Shklyar, H. Lenske, and U. Mosel, *Phys. Rev. C* **72**, 015210 (2005).
- [37] C. Hanhart and K. Nakayama, *Phys. Lett. B* **454**, 176 (1999).
- [38] V. Baru, A. M. Gasparyan, J. Haidenbauer, C. Hanhart, A. E. Kudryavtsev, and J. Speth, *Phys. Rev. C* **67**, 024002 (2003).
- [39] Y. Dong, A. Faessler, T. Gutsche, and V. E. Lyubovitskij, *Phys. Rev. D* **90**, 094001 (2014).
- [40] J. Haidenbauer and G. Krein, *Phys. Lett. B* **687**, 314 (2010).